5-15-2014

Directional Selective Neurons In Awake LGN: Response Properties And Modulation By Brain State

Xiaojuan Hei
University of Connecticut - Storrs, xiaojuan.hei@uconn.edu

Directional Selective Neurons in Awake LGN: Response Properties and Modulation by Brain State

Xiaojuan Hei

B.S., Xi'an Jiaotong University, Xi'an, China, 2009

A Thesis

Submitted in Partial Fulfillment of the

Requirements for the Degree of

Master of Arts

at the

University of Connecticut

2014

APPROVAL PAGE

Master of Arts Thesis

Directional Selective Neurons in Awake LGN: Response Properties and Modulation by Brain State

Presented by

Xiaojuan Hei, B.S.

Major Advisor _____
Harvey A. Swadlow, Ph.D.

Associate Advisor _____
Jose-Manuel Alonso, Ph.D.

Associate Advisor _____
Maxim Volgushev, Ph.D.

University of Connecticut

2014

ACKNOWLEDGEMENTS

I would like to give my special thanks to my major advisor, Dr. Harvey A. Swadlow, for his invaluable insights and guidance on this project and thesis. I would also like to thank my committee members Dr. Jose-Manuel Alonso and Dr. Maxim Volgushev for their helpful suggestions and discussions. In addition, I would like to thank my lab mates, Dr. Yulia Bereshpolova, Dr. Carl Stoezel, Dr. Jun Zhuang, Mr. Joseph Huff and Mr. Victor Serdyukov for their help on experiment surgery, data collection and analyses and software and hardware support.

TABLE OF CONTENTS

List of figures

Abstract

Directionally selective (DS) neurons are found in the retina and lateral geniculate nucleus (LGN) of rabbits and rodents. In rabbits, LGN DS cells project to primary visual cortex. Here, we compare visual response properties of LGN DS neurons with those of layer 4 simple cells, most of which show strong direction/orientation selectivity. The response properties of these populations differed dramatically, suggesting that DS cells may not contribute significantly to the synthesis of simple receptive fields: (a) whereas the F1/F0 ratios of LGN DS cells are strongly nonlinear, those of simple cells are strongly linear, (b) whereas LGN DS cells have overlapped ON/OFF subfields, simple cells have either a single ON or OFF subfield, or two spatially separate subfields, and (c) whereas the preferred directions of LGN DS cells are closely tied to the four cardinal directions, the directional preferences of simple cells are more evenly distributed. We further show that directional selectivity in LGN DS neurons is strongly enhanced by alertness via two mechanisms, (a) an increase in responses to stimulation in the preferred direction and (b) an enhanced suppression of responses to stimuli moving in the null direction. Finally, our simulations show that these two consequences of alertness could each serve, in a vector-based population code, to hasten the computation of stimulus direction when rabbits become alert.

Introduction

In rabbits and rodents, computing the direction of visual motion begins in the retina, where directionally selective (DS) ganglion cells project to brainstem targets and the visual thalamus (Stewart et al., 1971; Simpson, 1984; Huberman et al., 2009). Whereas most DS ganglion cells respond in spatially overlapping zones to both light onset and offset, some respond only to light onset (Barlow et al., 1964). Mechanisms underlying directional selectivity in retinal ganglion cells (Demb, 2007) have been studied intensively in rabbits (eg., Fried et al., 2002, 2005; Oesch et al., 2005) and, more recently in transgenic mice (Yoshida et al., 2001; Weng et al., 2005; Huberman et al., 2009). Whereas brainstem projections of retinal DS neurons control aspects of eye position (Simpson, 1984; Cavanaugh et al., 2012), little is known about the function of the projections of retinal DS neurons to thalamocortical circuits. We have previously shown (Swadlow and Weyand, 1985) that DS neurons in rabbit LGN do project to the primary visual cortex (V1), that their axons are fast-conducting (similar to those of concentrically organized LGN cells), and that LGN DS neurons are much more prevalent in the representation of the upper visual field (dorsal portion of the LGN) than in the representation the visual streak (the region of high receptor and ganglion cell density representing vision along the horizon, Hughes, 1971). Moreover we have recently found that at least some of the LGN DS neurons provide a synaptic input to layer 4 of V1 (Hei et al., 2013). However, the manner in which LGN DS neurons contribute to the processing of information in V1, are unknown.

Here, we target DS neurons in the LGN representation of the visual streak of awake rabbits, and compare their properties with layer 4 cortical neurons recently studied in the corresponding region of primary visual cortex (V1, Zhuang et al., 2013). We examined the visual response properties of LGN DS neurons, and showed that their responses are highly non-linear, consist of highly overlapping ON and OFF subfields, and that their preferred directions are, like their

counterparts in the retina (Oyster and Barlow, 1967), restricted to the four cardinal directions. Notably, each of these visual response properties are dramatically distinct from those of V1 layer 4 simple cells studied in the same preparation using identical methods (Zhuang et al., 2013), suggesting that LGN DS neurons do not contribute strongly to the synthesis of the direction/orientation selectivity seen in V1 simple cells. Next, we show that the visual responses of LGN DS cells are strongly modulated by alertness, which increases responses in the preferred direction and suppress responses in the null direction, making them more directional selective. Finally, we present a simple model and simulations that show how the response changes seen in LGN DS cells during alertness could result in faster computation of stimulus direction by a vector based population code.

Materials and Methods

Extracellular single unit recordings were made in the LGN from five awake adult female Dutch-Belted rabbits. The general surgical procedures have been reported previously (Swadlow, 1991; Swadlow et al., 1998; Stoelzel et al., 2008; Bereshpolova et al., 2011; Zhuang et al., 2013) and are briefly descried here. All experiments were conducted under the approval of the University of Connecticut Animal Care and Use Committee in accordance with National Institutes of Health guidelines.

Animal preparation.

Initial surgery was performed under ketamine-acepromazine anesthesia using aseptic procedures. Stainless steel screws were installed on the dorsal surface of the skull and fused together with acrylic cement after removing skin and fascia. A stainless steel rod oriented in a rostrocaudal direction was cemented to the acrylic mass. This rod held the rabbit rigidly during electrode implantation and recording sessions. Silicone rubber was used to buffer the wound margins from the acrylic cement on the skull. After at least 10 days of recovery, neuronal activity recordings were obtained from awake rabbit through a small hole in the skull.

Electrophysiological recordings.

All the electrophysiological recordings were acquired by Plexon data acquisition system (Plexon Corp., Dallas, Texas). Single unit recordings from LGN of awake rabbit were obtained using a chronically implanted seven-channel system (Swadlow, 2005) with seven sharp-tip quartz-insulated platinum/tungstren (1.5-3 Mohm) electrodes organized concentrically and each

independently controlled by a miniature microdrive. Multi-unit recordings from superficial layers of superior colliculus (SC) were obtained using a three-channel system similar to the LGN system but with low impedance (<1.5 Mohm) electrodes. Hippocampal EEG and cortical EEG were simultaneously recorded with platinum-iridium microwires for monitoring brain states (Bezdudnaya et al., 2006; Bereshpolova et al., 2011; Zhuang et al., 2013).

Receptive field and visual stimulation.

Receptive fields were plotted for the LGN cells under study and mapped by reverse correlation (Jones and Palmer, 1987; Stoelzel et al., 2008) using sparse noise stimuli made of white and black squares (1-2˚; 10-20 ms), which were pseudorandomly presented on a primary monitor (40x30 cm, 48 cd/m^2 mean luminance, 160 Hz refresh rate). Eye movements were monitored by constant tracking of SC multi unit activity and using an infrared eye camera system (see *Monitoring eye position* for details). Cells' receptive field properties were tested using sine-wave drifting grating stimulation with optimal parameters (size, temporal frequency, spatial frequency, orientation/direction and contrast). The orientation/directional tuning was measured with gratings drifting in one of the 8, 12 or 24 randomly interleaved directions while keeping other parameters optimal. Spatial frequency tuning was tested from 0.00825 to 1.32 cycles per degree (cpd) while keeping other parameters optimal. Each presentation lasted 3-8 s with 2 s gaps in between (mid-luminance screen was shown to the animal during the gaps). The mean presentation number per condition was 190.4 ± 7.68. For some cells, spontaneous activity was also recorded using a screen with mid-luminance.

Cell classification.

After an LGN cell was identified, circular drifting gratings were used to determine if a cell was directionally selective, based on their strong selectivity to the direction of motion. A direction selective index (DSI, see below for definition) was calculated and only cells with DSI more than 0.4 were considered as DS cells.

We generally studied only DS neurons, but in some cases we compared DS neurons with concentrically organized LGN cells. Concentric cells showed strong surround inhibition with no or very poor orientation selectivity. They were further classified as sustained or transient concentric cells based on their responses to stationary white or black spots, which were presented on the cell's receptive field center for 2 s with 2 s gaps between stimulation. The spots were chosen to match the size and sign of the receptive field center.

Search strategy for LGN DS cells.

All LGN cells studied here had receptive fields in the monocular region of visual space, 20 ˚-110 ˚from the midline (0 ˚being in front of the animal), at an elevation of +15 ˚to -5 ˚from the horizontal. This retinotopic region roughly corresponds to the region of maximal receptor and ganglion cell density in rabbit retina (the visual streak, Hughes, 1971), and DS neurons are relatively rare in this retinotopic region of the LGN. Thus, Stoelzel et al. (2008) reported only 2/83 (2.4%) DS neurons with receptive fields in this region of visual space. Similarly, Swadlow and Weyand (1985) found only 3.4% LGN DS neurons at elevations of -5 to +15 degrees, but found 17.8% DS neurons at elevations > 15 degrees (recalculated from the original data set presented in Fig. 5 of Swadlow and Weyand, 1985). Nevertheless, we chose to limit our analysis of DS neurons to the representation of visual streak in order to be able to compare

these cells with V1 simple cells studied in this region of visual space (Zhuang et al., 2013; Zhuang et al., 2014). To achieve this, our strategy was to limit, as much as possible, recordings to DS neurons. This was accomplished by quickly abandoning non-DS neurons following brief visual testing (i.e. neurons that showed roughly equivalent responses to movement in multiple directions around the four cardinal directions were discarded).

Monitoring eye position.

The rabbits generally have very stable eyes and often keep their eye position within ± 0.5˚ for up to several minutes (Collewijn, 1971; Swadlow and Weyand, 1985; Bezdudnaya et al., 2006). During each recording session, the SC multi unit receptive field positions were mapped with sparse noise stimuli on a secondary LCD monitor (Acer AL1515, 23 x 20 cm, 36 cd/m^2 mean luminance, 75 Hz refresh rate). The relationship between the SC and LGN receptive field center positions was set up during the mapping process when the rabbit's eye was stable. Once an eye movement occurred during the visual stimulation, the stimulus was dynamically moved to be centered on the LGN receptive field center based on this relationship. At the same time, for most cells, the pupil position and size were monitored by an infrared camera system (ViewPoint EyeTracker system, Arrington Research, Inc.), which was ~ 40 cm away from the rabbit eye. Data recorded ± 15 sec of an eye movement were discarded during offline analysis and only data recorded during eye stable periods are reported here.

EEG Brain States.

The data were segmented into two distinct brain states, alert state and non-alert state, based on the simultaneously recorded hippocampal EEG and cortical EEG activity. The alert state was defined as hippocampal theta activity (5-7 Hz) and cortical desynchronization, while non-alert state was defined as high voltage irregular hippocampal activity and cortical synchronization. Sometimes, novel non-visual stimulations (e.g. random sounds, tactile stimulation) were applied to arouse the animal from non-alert to alert states. Power spectrum density graphs were generated for each cell to verify the states separation. Data reported here for alert state range from 14 to 65% of the time that the cells were studied (mean: 33 ± 2.4%) and for non-alert state from 13-54% (mean: 31 ± 2.1%). The remaining portions of the data sets (36%, on average) could not be classified unambiguously as either alert or non-alert and were not included in the state analyses.

Data Analysis.

Spike waveforms were identified online and verified offline by Plexon cluster analysis software. All data were then analyzed by Plexon NeuroExplorer (Nex Technologies, Inc.) and MATLAB (The MathWorks, Inc.).

Data of the first two cycles of each presentation were removed to discard transient responses to stimulus onset. Then using Fourier analysis, the mean firing rate (F0) and first harmonic component (F1) of PSTH graphs were calculated for further analysis. Unlike concentric cells in the LGN, which respond to a drifting grating with strong modulations of the temporal frequency tested (F1 modulation), the DS cells responded mainly with an increase in the mean firing rate (F0). F1 modulations were hardly seen in LGN DS cells (see below for one exception). So, except for measurements of spatial frequency tuning, all other measurements are reported as F0 responses only (total firing rate, spontaneous rate was not subtracted).

Statistical significance was determined by independent sample t test, unless otherwise stated. Mean and standard error are represented for figures with bar graphs (*: p<0.05; **: p<0.01; ***: p<0.001).

Receptive field structure.

The receptive field structure was measured by reverse correlation (Jones and Palmer, 1987; Stoelzel et al., 2008) with sparse noise stimuli and ON/OFF receptive field matrices were generated with a 20 ms time window around the peak response. The matrices were smoothed with a Gaussian filter and a 30% threshold was applied. Contour plot lines were fitted using bicubic interpolation and each line represents a 10% decrement. To measure the overlap between ON and OFF responses, the local similarity index (LSI) was calculated as follows:

$$LSI = \sum(RF_{ON} * RF_{OFF}) / \sqrt{\sum(RF_{ON} * RF_{ON}) * \sum(RF_{OFF} * RF_{OFF)}}$$

RF_{ON} and RF_{OFF} are the ON and OFF receptive field matrices after applying the filter and threshold. The values of LSI range from 0 to 1. LSI equals 1 when ON and OFF receptive fields totally overlap with each other and equals 0 when they are entirely separated.

Directional tuning

Directional tuning for each cell was measured as the average of F0 responses measured with gratings pseudorandomly drifting in 8, 12 or 24 directions. For each cell, the preferred direction, direction selective index (DSI), orientation selective index (OSI) and circular variances were calculated. The preferred direction was computed as the vector sum of the responses in all the directions. The DSI, OSI, circular variance for DSI (CVd) (Grabska-Barwinska et al., 2012) and circular variance for OSI (CVo) (Ringach et al., 2002) were calculated as follows:

$$DSI = (R_{pref} - R_{null})/(R_{pref} + R_{null})$$

$$OSI = (R_{pref} - R_{orth})/(R_{pref} + R_{orth})$$

$$CVd = \left|\sum R_j e^{i\theta_j}/\sum R_j\right|$$

$$CVo = \left|\sum R_j e^{i2\theta_j}/\sum R_j\right|$$

where R_{pref} is the F0 response in the measured preferred direction, which was defined as the stimulus direction closest to the vector sum of responses across all directions. R_{null} is the F0 response in the stimulus direction 180° opposite of the preferred direction; $R_{orth}$is the averaged F0 response in the stimulus directions 90° away from the preferred direction; j represents all the directions tested, R_j and θ_j are the F0 responses and angles (in radians) in j^{th} direction. DSI, OSI, CVd and CVo range from 0 to 1; all of them approach 1 in neurons with strong direction or orientation selectivity and approach 0 in neurons with poor direction or orientation selectivity. DSI and OSI only take the responses from two or three points of the tuning curve into account, while CVd and CVo measure the index from all the points of the tuning curve and are more robust. Only cells with DSI > 0.4 were considered as direction selective cells.

The tuning curve of each cell was fitted by the von Mises distribution, modified from Elstrott et al. (Elstrott et al., 2008):

$$R = R0 + R_{max} e^{kcos(x-\mu)}/e^k$$

where R is the F0 response in any given direction x; Rmax is the maximum F0 response; μ is the preferred direction in radians and k is the concentration parameter for tuning width. The half tuning width at half height (HWHH) of the fitted tuning curve was measured as follows:

$$HWHH = \theta = \text{acos}(\ln(0.5 * e^{k} + 0.5 * e^{-k}) / k)$$

This HWHH parameter shows the sharpness of the orientation/directional tuning.

***Spatial frequency and response linearity*.**

Spatial frequency tuning responses were measured with grating's spatial frequency ranging from 0.00825 to 1.32 cycles per degree (cpd) (for some cells: 0.05 to 1.32 cpd). For measuring the response linearity, spatial frequency tuning of both F0 and F1 responses were measured and analyzed. The tuning curves were fitted by Gaussian model:

$$y = R_0 + R_{sf} * e^{(-(x-SF_{peak})^2/2{\sigma_{sf}}^2)}$$

where y is the F0 or F1 response to each spatial frequency (x) tested, R_0 is the baseline activity, SF_{peak} is the spatial frequency that elicits the maximum response (R_{sf},), σ_{sf} is the standard deviation of the spatial tuning curve (the width of the Gaussian function). Here, the sum of R_0 and R_{sf} was considered as the peak F0 or peak F1 response.

To measure cell's response linearity, F1/F0 ratio was calculated. Since the spatial frequencies that elicited the strongest F0 and F1 responses were not always the same, we implemented a previously described method (De Valois et al., 1982; Chen et al., 2009) to calculate it. First, we selected the three spatial frequencies that generated the largest combined F1 and F0 responses. Then, we obtained the F1/F0 ratio by averaging the F1 and F0 responses for these three spatial frequencies. So the F1/F0 ratio is represented by F1 average/F0 average ratio.

LGN DS simulation

In order to understand the alert and non-alert state effect on LGN DS cells, we built a model to simulate the response properties of LGN DS neurons. To get the population tuning curve for the simulation, we normalized each cell's tuning curve in both alert and non-alert states by the maximum mean firing rate in the alert state. Then, the normalized tuning curves were aligned by their preferred directions and multiplied by the population average of firing rates in the preferred direction in the alert state of all the cells to obtain the population average of the tuning curves. We simulated 4 LGN DS cells tuned to each of the four cardinal directions. Each of these cells had identical tuning curve shapes as the population average, but different preferred directions: anterior, superior, posterior and inferior, respectively.

The mean firing rates of the four simulated DS cells to a particular stimulus direction (Stim Direc) were extracted from their tuning curves to generate spike trains for each cell by Poisson process. The integration time of the spike trains was gradually increased from 10 ms to 0.5 s with a 10 ms step. For each DS cell, the spike rates were calculated for each integration time. These firing rates were provided to a vector sum detector, which compares the vector sum from the calculated firing rates to the vector sum from the tuning curves. The direction which gave the minimal difference between these two vector sums was considered as the predicted stimulus direction (PD). Then the relationships between the integration time and the mean predicted error (differences between the Stim Direc and PD) were plotted for the alert, non-alert and non-alert scaled (the non-alert state tuning curve was scaled to the maximum firing rate of the alert state) states. A thousand simulation iterations were performed for each cell in each condition.

Results

Nineteen DS cells were recorded from five awake Dutch-Belted rabbits. Drifting gratings were presented over their receptive field center, and were optimally matched in size, temporal frequency, spatial frequency, luminance contrast, and then the orientation/direction was randomly changed to test 8, 12 or 24 directions.

The orientation/directional tuning of one example DS cell is shown in **Fig. 1**. The cell was tested under drifting grating stimuli that has parameters of 5 degrees in size, 16 Hz in temporal frequency of 16; 0.132 cycle per degree in spatial frequency and 73% in contrast. Black dots represent the F0 responses in the grating directions tested. Solid curve and dashed circle show the fitted tuning curve and spontaneous firing rate, respectively. Peristimulus time histograms (PSTHs) in two cycles of stimulation each are shown for 12 of the tested directions. For this particular example, when the drifting grating was moving from posterior to anterior direction, the cell fired vigorously and maximally, especially compared with the response when the stimulus moved in the opposite direction, the anterior to posterior direction, where the cell showed minimal firing. Note that the response in the anterior direction is lower than the spontaneous firing rate (marked as a small dotted circle at the center of the plot).

Figure 1

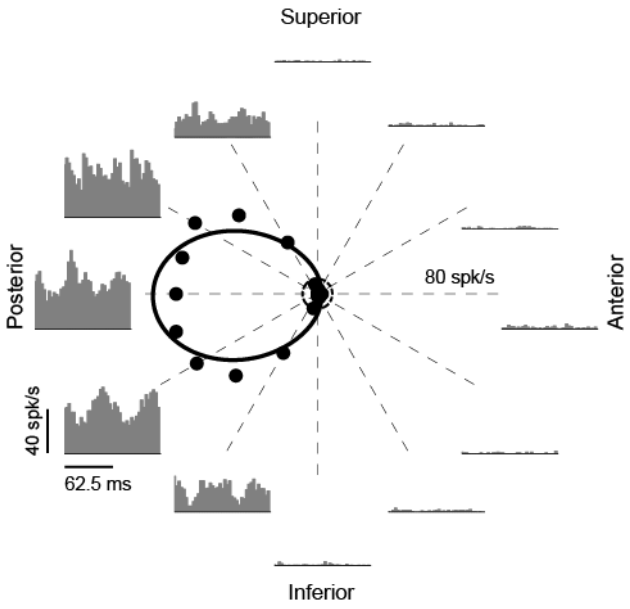

Figure 1. Orientation/directional tuning of one LGN direction selective cell. Each black dot shows the F0 response for each particular stimulus direction. Solid curve is the fitted curve by von Mises function and dashed circle represents the spontaneous firing rate. PSTHs (two cycles) are shown for 12 tested directions.

Receptive field properties of DS cells in LGN and comparison with simple cells

LGN DS cells, which have been shown previously by antidromic activation, send their fast conducting axons to the primary visual cortex (V1) (Swadlow and Weyand, 1985), and at least some provide a strong input to layer 4 (Hei et al., 2013). Since layer 4 in V1 receives a bulk of thalamic input from LGN (Stoelzel et al., 2008) and simple cells in layer 4 exhibit strong orientation/direction selectivity (Zhuang et al., 2013), we compare the receptive field properties of LGN DS cells and layer 4 simple cells (**Fig. 2 B, D, E, F**).

Unlike LGN cells with concentric receptive fields, which have either pure ON or pure OFF receptive field centers (Swadlow and Weyand, 1985), LGN DS cells all had overlapped ON/OFF receptive field subregions (**Fig. 2A**). To measure the degree of overlapping between ON and OFF receptive field subregions, a local similarity index (LSI) was calculated for LGN DS, LGN concentric cells and simple cells. The distribution of LSIs for each class is shown in **Fig. 2B**. LSI ranges from 0 to 1, with 0 meaning no overlap between ON and OFF subfields and 1 meaning complete overlap (see methods). The distribution of LSI for DS cells and concentric cells are significantly bimodal (Hartigan's test, $P<0.001$) with the LSI for all DS cells being more than 0.35 (mean = 0.75 ± 0.04, **Fig. 2B**, black) and LSI for concentric cells less than 0.02 (mean = 0.0009 ± 0.0009, most of them have LSI equals 0, **Fig. 2B**, grey). Simple cells have pure ON or pure OFF or segregated ON/OFF receptive fields (Zhuang et al., 2013), so it is not surprising to see a significant difference of LSI between LGN DS and layer 4 simple cells (mean: DS vs. simple: 0.75 ± 0.04 vs. 0.03 ± 0.007, $p<0.001$, **Fig. 2B**). The distribution of LSIs for LGN DS and layer 4 simple cells is also significantly bimodal (Hartigan's test, $p<0.01$).

The preferred direction responses of LGN DS neurons are nearly 10 times of the responses in the null direction (180 degrees opposite of the preferred direction), (mean: preferred vs. null:

39.58 ± 4.3 vs. 4.07 ± 1.1 spikes/s, paired t-test, *p<0.001*, **Fig. 2C**, population averages are shown in the inset).

To quantify the cells' direction selectivity, both direction selectivity index (DSI) and circular variance for DSI (CVd) were computed. DSIs were calculated based on the preferred and null direction responses (see methods) and was close to 1 in cells with strong direction selectivity and close to 0 in cells with poor direction selectivity. As noted in methods, only LGN cells with DSIs of > 0.4 were classified as DS cells, and the distributions of DSIs for all LGN DS (black) and simple (white) cells are shown in **Fig. 2D**. Note that most of the simple cells are very direction selective (47 out of 56 cells have DSI > 0.4). We also calculated the CVd, which is based on the entire orientation/directional tuning curve (see methods) and ranges from 0 to 1, with larger values representing shaper directional tuning. The distribution of CVd of LGN DS cells ranged from 0.2 to 0.8 (mean: 0.56 ± 0.04) (**Fig. 2D inset, black**) suggesting that some DS cells are relatively more sharply tuned than others. The CVds for simple cells (**Fig. 2D**, white) are similar to that of LGN DS cells (mean: simple: 0.49 ± 0.03, *p=0.144*). Orientation selectivity index (OSI) and circular variance for orientation (CVo) were also computed to quantify the cells' orientation selectivity. The value of OSI and CVo, as for DSI and CVd, range from 0 to 1, with values close to 0 representing poor orientation selectivity and those close to 1 representing strong orientation selectivity. Cortical simple cells had better orientation selectivity than LGN DS cells, as measured by CVo (**Fig. 2E,** OSI: mean: LGN DS vs. simple: 0.67 ± 0.05 vs. 0.8 ± 0.05, *p=0.072*; CVo: mean: LGN DS vs. simple: 0.24 ± 0.03 vs. 0.47 ± 0.03, *p<0.05)*.

The preferred direction of each cell was calculated by vector sum and the distribution is shown in **Fig. 2F**. It is very obvious that the distribution of LGN DS cells' preferred directions (black) forms four groups (Anterior, Posterior, Superior and Inferior), resembling the distribution of ON_OFF direction selective ganglion cells in the rabbit retina (Oyster and Barlow, 1967). In contrast, the preferred directions of cortical simple cells (red) are more homogeneously

distributed. LGN DS cells are much more likely to prefer movement in the directions within 15 degrees of cardinal axes than are simple cells (mean: DS vs. simple: 17 out of 19 vs. 27 out of 54, X^2 test, *p=0.002*, **Fig. 2F**). This suggests that, compared to simple cells, LGN DS cells better code movements in the four directions, anterior, posterior, inferior and superior.

Normalized and averaged population tuning curves are shown for each of the four cardinal groups (green: anterior population, n=7; black: superior population, n=2; cyan: posterior population, n=5; magenta: inferior population, n=5; error bar: standard error, **Fig. 2G**). The LGN DS cells are relatively broadly tuned with four prominent peaks in the four cardinal directions (tuning curves are superimposed together from **Fig. 2G**, **Fig. 2H**).

Figure 2

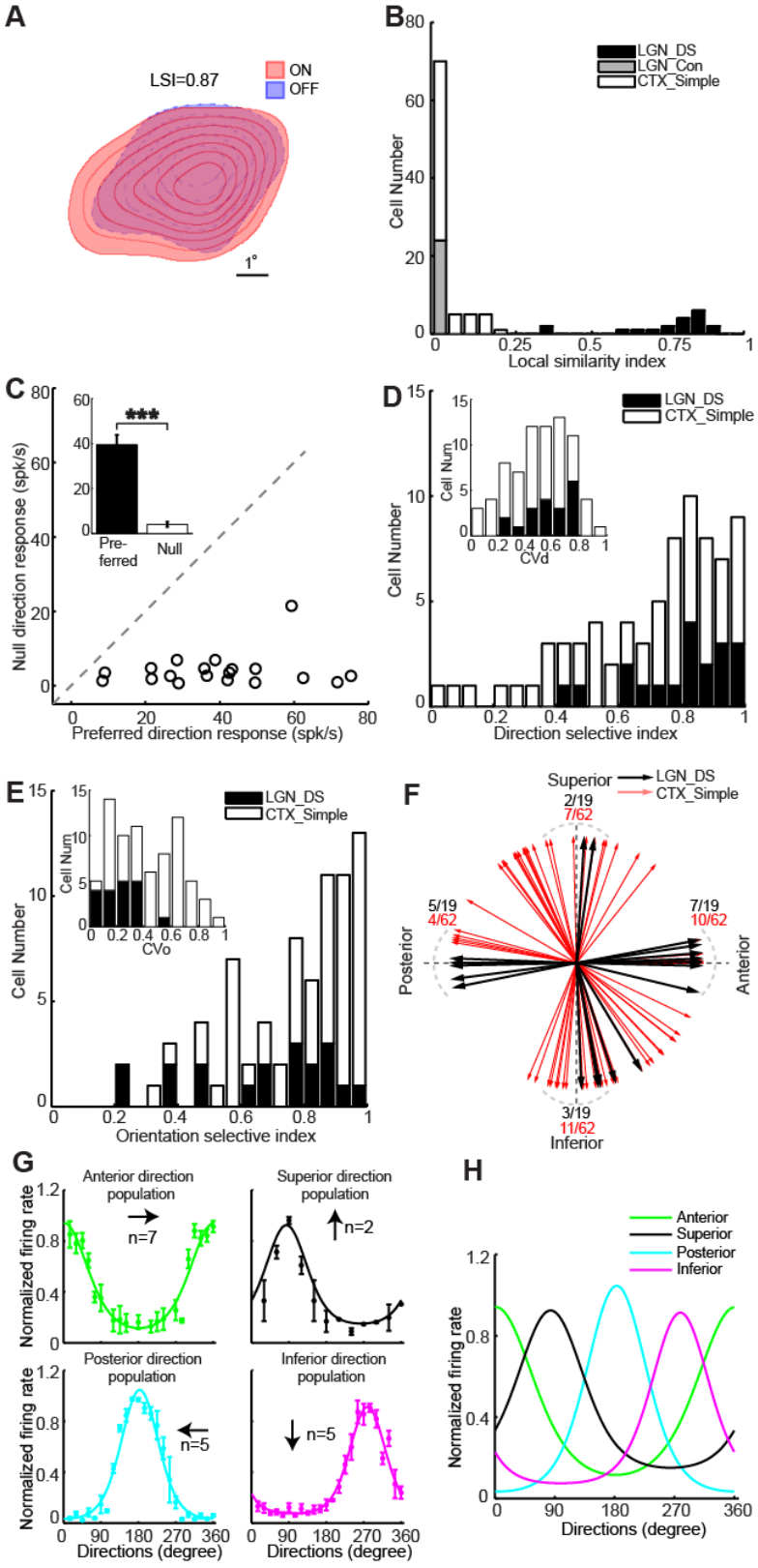
A
LSI=0.87
ON
OFF
1°
B
LGN_DS
LGN_Con
CTX_Simple
Cell Number
Local similarity index
C
***
Pre-ferred
Null
Null direction response (spk/s)
Preferred direction response (spk/s)
D
LGN_DS
CTX_Simple
Cell Num
CVd
Cell Number
Direction selective index
E
LGN_DS
CTX_Simple
Cell Num
CVo
Cell Number
Orientation selective index
F
Superior
LGN_DS
CTX_Simple
2/19
7/62
5/19
4/62
7/19
10/62
3/19
11/62
Posterior
Anterior
Inferior
G
Anterior direction population
n=7
Superior direction population
n=2
Posterior direction population
n=5
Inferior direction population
n=5
Normalized firing rate
Directions (degree)
H
Anterior
Superior
Posterior
Inferior
Normalized firing rate
Directions (degree)

Figure 2. Receptive field properties of LGN DS and cells with concentric receptive fields in the LGN (Data for layer 4 simple cells were reanalyzed from Zhuang et, al., 2013). **A,** Receptive field map of the direction selective cell show in **Fig.1**. **B,** Distribution of local similarity index for direction selective cells (LGN_DS, black), concentric cells (LGN_Con, gray) in LGN and simple cells (CTX_Simple, white) in layer 4 of V1. **C,** Relationship between responses in the preferred direction and null direction of LGN direction selective cells. Inset shows the population average. **D,** Distribution of direction selectivity index of LGN direction selective cells (LGN_DS, black) and layer 4 simple cells (CTX_Simple, white). Inset: Distribution of circular variance for DSI. **E,** Distribution of orientation selectivity index (LGN DS in black and layer 4 simple cells in white). Inset: Distribution of circular variance for OSI. **F,** Distribution of preferred directions of LGN direction selective cells (black arrow) and layer 4 simple cells (red arrow). 15 degrees around cardinal axes are represented by gray dashed curves. Number of cells fall into those directions is indicated by numbers (LGN DS, black; simple, red). **G,** Normalized population curves for anterior (n=7, green), superior (n=2, black), posterior (n=5, cyan) and inferior (n=5, magenta) directions. Normalized and averaged data points are represented in dots with standard error represented by error bars. The smoothed curves are fitted curve by von Mises function. **H,** Superimposed directional tuning curves for the four directions.

The linearity of spatial summation

Spatial frequency tunings of 10 LGN DS cells and 20 concentric cells were tested and each frequency was examined for both the F0 and F1 responses. Orientation/directional tuning curve for one example DS cell is shown in **Fig. 3A** and the corresponding spatial frequency tuning curve in **Fig. 3B**, respectively. Dots are the responses measured under different spatial frequencies, and solid and dashed curves are the fitted curves of F0 and F1 responses by the Gaussian model (see methods). Nine of 10 LGN DS cells had higher F0 responses than F1 responses at ALL of the spatial frequencies tested (e.g. **Fig. 3B**), however, one LGN DS cells had higher F0 responses at high spatial frequencies and higher F1 responses at low spatial frequencies (data not shown). In the population of LGN DS cells studied, all but one cell (9 out of 10) had higher peak F0 response than peak F1 response (The exception is indicated by the grey arrow) (**Fig. 3C**). Population averages are shown in the inset of **Fig. 3C**.

F1/F0 ratio is a common way to classify simple and complex cells in the cortex with simple cells having F1/F0 > 1 and complex cells F1/F0 < 1 (Movshon et al., 1978). To better compare the linearity of LGN DS, LGN concentric and V1 simple cells, we also calculated the F1/F0 ratios to drifting grating stimulation. We chose the three spatial frequencies that elicited the maximum combined F0 and F1 responses. Then, we calculated the F1/F0 ratio by averaging the F1 and F0 responses for these three spatial frequencies. The F1/F0 ratios for all but one DS cells were less than 0.4 (mean for all the DS cells with F1/F0 < 1: 0.24 ± 0.029). By contrast, 18 out of 20 LGN concentric cells and 40 out of 44 layer 4 simple cells had F1/F0 greater than 1 (mean for all LGN concentric cells: 1.41 ± 0.27; mean for all V1 simple cells: 1.46 ± 0.048, LGN DS vs. simple: $p<0.01$, LGN DS vs. LGN concentric: $p< 0.05$, **Fig. 3D**). The LGN DS cell that has F1/F0 ratio >1 is indicated by the gray arrow (**Fig. 3D**). Therefore, LGN DS are much more nonlinear compared to LGN concentric cells and layer 4 simple cells.

Figure 3

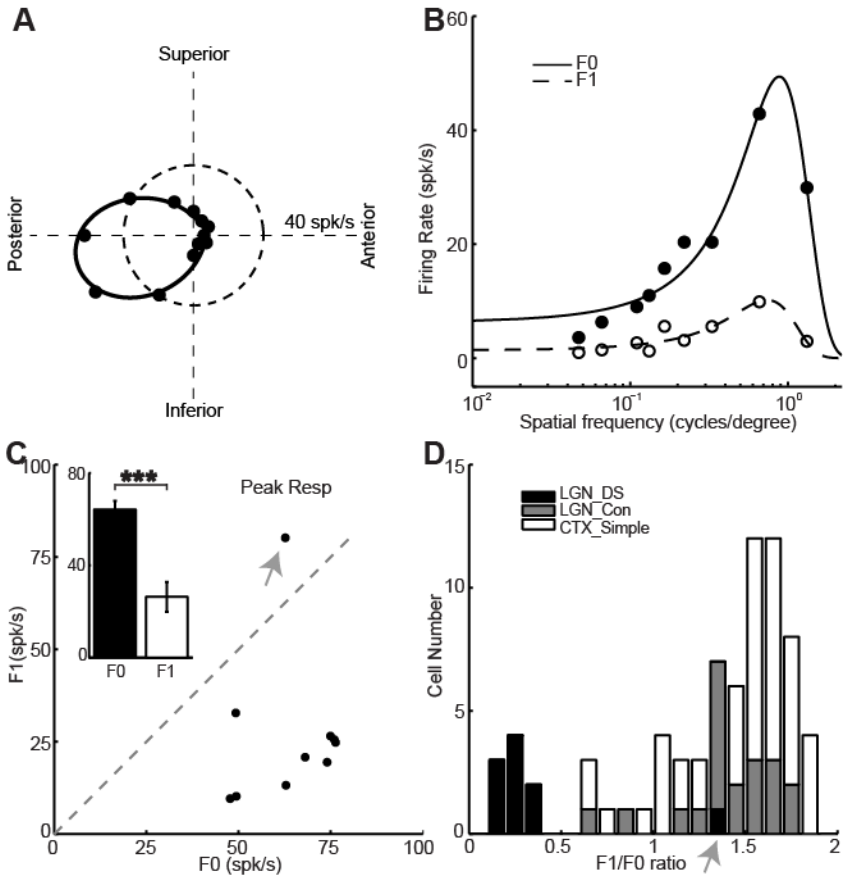

Figure 3. Spatial tuning properties and linearity of LGN direction selective cells and layer 4 simple cells. **A,** Orientation/directional tuning of one direction selective cell. **B,** Spatial frequency tuning curves for cell in (**A**). F0 responses are represented by closed dots and solid fitted curves; F1 responses are indicated by open dots and dashed fitted curves. **C,** The relationship between peak F0 response (x axis) of spatial frequency tuning and peak F1 response (y axis) of LGN direction selective cells. Inset: peak F0 responses are significantly higher than peak F1 responses. **D,** Distribution of F1/F0 ratios for LNG DS, LGN concentric cells and simple cells. The gray arrows in (**C**) and (**D**) indicate an exception cell which has higher F1 responses than F0 responses.

Response modulations by brain state

Awake rabbits shift between alert and non-alert states both spontaneously, and in response to diverse sensory stimulation. Notably, this shift in brain state is associated with profound changes in LGN and V1 responses. We have previously shown that LGN concentric cells have higher spontaneous firing rate, lower burst rate and higher response gain in the alert state than in the non-alert state (Bezdudnaya et al., 2006; Cano et al., 2006; Bereshpolova et al., 2011). Like LGN concentric cells, here we show that DS cells also have significantly higher spontaneous firing rates and lower burst rate in the alert state (mean spontaneous firing rate: alert vs. non-alert: 15.36 ± 1 vs. 9.95 ± 0.95 spikes/s, paired t test, *p<0.001*, **Fig. 4A**; mean burst rate: alert vs. non-alert: 0.17 ± 0.04 vs. 2.42 ± 0.31 bursts/s, paired t test, *p<0.001*, **Fig. 4B**). Alertness also increased the visual responses of LGN DS cells selectively around their preferred direction of movement and had an opposite suppressive effect around the null direction (**Fig. 5**). LGN DS cells generated stronger responses during the alert (**Fig. 5A**) than non-alert (**Fig. 5B**) states and their spontaneous rates were also higher during the alert state (**Fig. 5C** dotted lines). However, the response to the non-preferred direction was weaker in the alert state (**Fig. 5C**). As a population (**Fig. 6**), alertness enhanced the visual responses of DS cells in the preferred direction and suppressed them in the null direction (mean response in the preferred direction: alert vs. non-alert: 51.73 ± 5.24 vs. 37.04 ± 6.21 spikes/s, paired t test, *p<0.01*, **Fig. 6A**; mean response in the null direction: alert vs. non-alert: 1.7 ± 0.62 vs. 4.24 ± 0.6 spikes/s, paired t test, *p<0.01*, **Fig. 6B**). As a consequence, the direction selectivity measured as both DSI and CVd also increased significantly in the alert state (mean for DSI: alert vs. non-alert: 0.93 ± 0.02 vs. 0.71 ± 0.07, paired t test, *p< 0.01*, **Fig. 6C;** mean for CVd: alert vs. non-alert: 0.64 ± 0.05 vs. 0.52 ± 0.06, paired t test, *p< 0.05*, **Fig. 6D**). Importantly, while the strength of the LGN DS visual responses could be strongly enhanced or suppressed by alertness, the orientation selectivity measured (OSI and CVo) and the tuning half width at half

height (HWHH) did not change with state (mean for OSI: alert vs. non-alert: 0.66 ± 0.08 vs. 0.64 ± 0.09, paired t test, *p=0.71*, **Fig. 6E**; mean for CVo: alert vs. non-alert: 0.24 ± 0.04 vs. 0.24 ± 0.05, paired t test, *p=0.881*, **Fig. 6F**; mean for HWHH: alert vs. non-alert: 56.45 ± 3.97 vs. 52.52 ± 4.49, paired t test, *p=0.3*, **Fig. 6G**).

In both states, visual responses in the null direction were strongly suppressed 2 to 8 times below the spontaneous firing rate (**Fig. 6H**, mean in the alert state: null vs. spontaneous: 1.85 ± 0.67 vs. 15.18 ± 1.15 spikes/s, *p< 0.001*; mean in the non-alert state: null vs. spontaneous: 4.51 ± 0.6 vs. 9.32 ± 0.85 spikes/s, *p<0.01*). Moreover, this response suppression in the null direction was ~ 2 times higher in the alert than non-alert states (mean: alert vs. non-alert: 87.98 ± 3.99 % vs. 45.45 ± 10.12%, *p<0.001*).

Figure 4

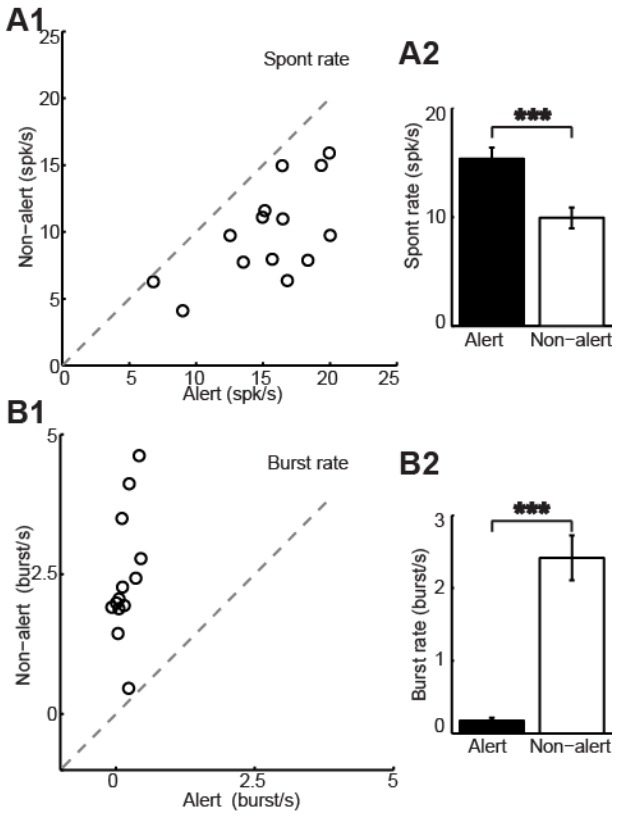

Figure 4. Brain state, spontaneous activity, and bursting of LGN DS cells. Spontaneous firing rate (**A**) is significantly higher, while burst rate (**B**) is significantly lower in the alert than in the non-alert state. **A2**, **B2**, are population averages (alert in black and non-alert in white).

Figure 5

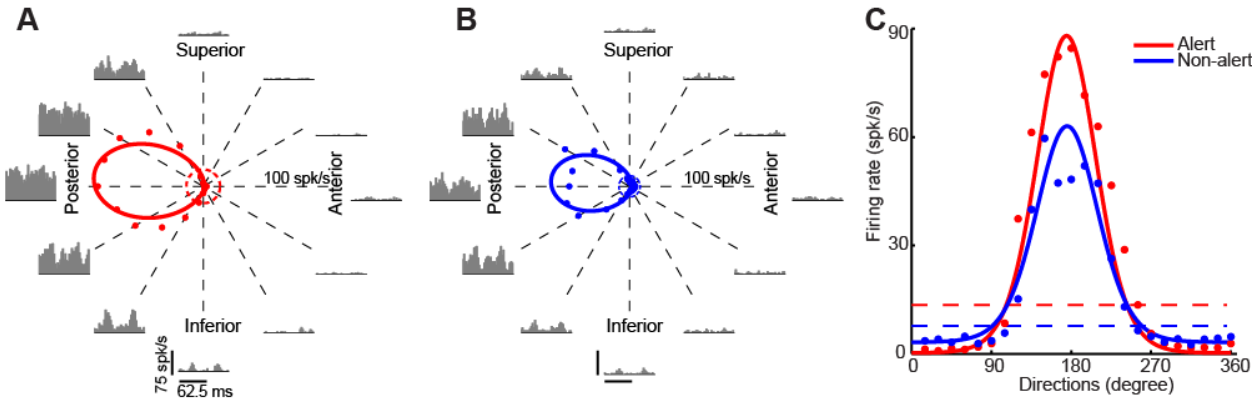

Figure 5. Brain state and orientation/directional tuning. The effects of brain state on one DS cell are shown. **A, B,** Tuning curves in alert (**A**) and non-alert (**B**) state with PSTHs shown for 12 different directions. Spontaneous rates are shown in dashed circles (alert in red, non-alert in blue). Notice the maximum axis in the tuning curve is 100 spikes/sec. **C,** The superimposed fitted tuning curves in alert (red) and non-alert (blue) state. Spontaneous firing rates are also shown in dashed lines.

Figure 6

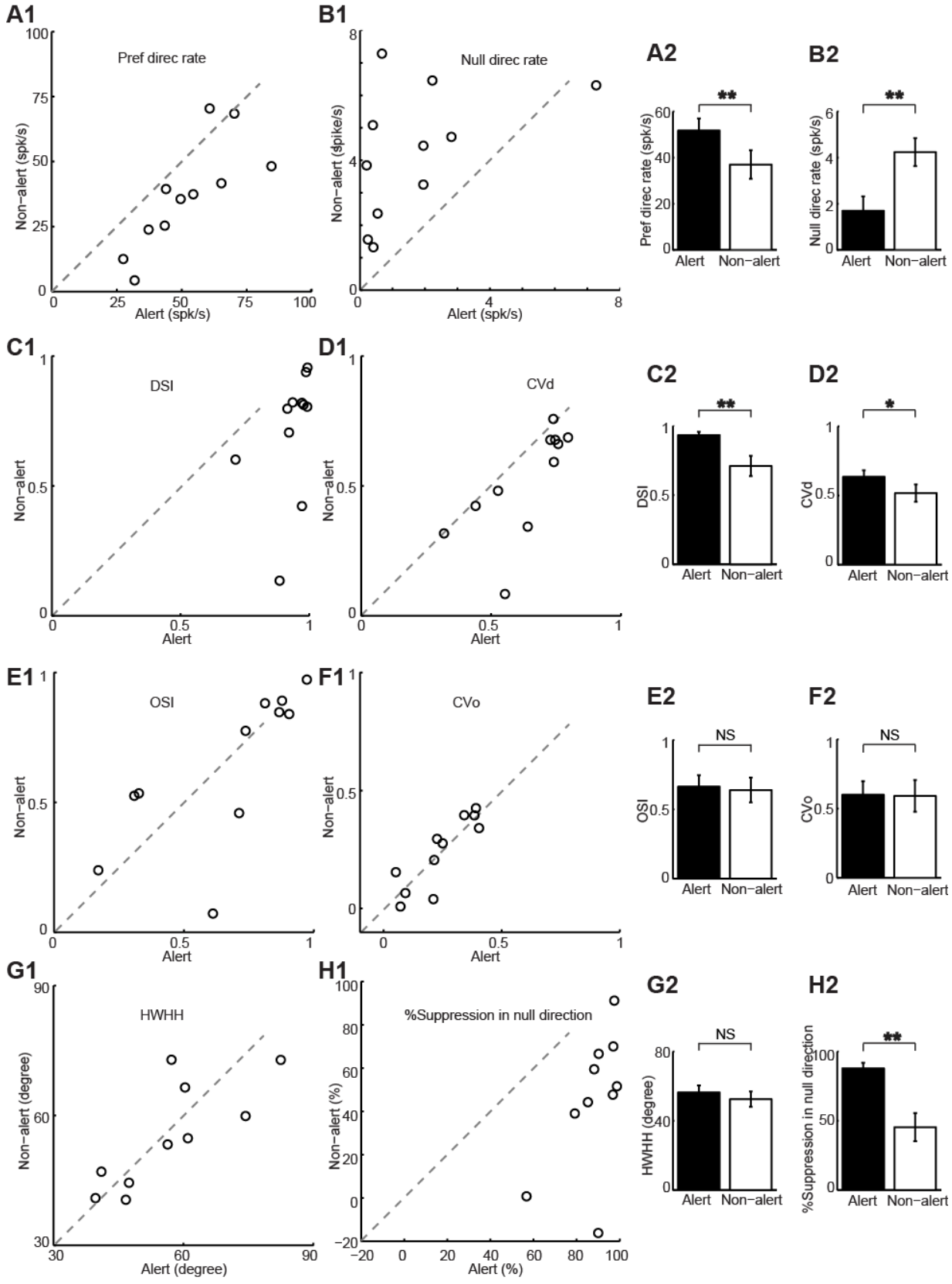
A1
Pref direc rate
Non−alert (spk/s)
Alert (spk/s)
B1
Null direc rate
Non−alert (spike/s)
Alert (spk/s)
A2
Pref direc rate (spk/s)
Alert
Non−alert
**
B2
Null direc rate (spk/s)
Alert
Non−alert
**
C1
DSI
Non−alert
Alert
D1
CVd
Non−alert
Alert
C2
DSI
Alert
Non−alert
**
D2
CVd
Alert
Non−alert
*
E1
OSI
Non−alert
Alert
F1
CVo
Non−alert
Alert
E2
OSI
Alert
Non−alert
NS
F2
CVo
Alert
Non−alert
NS
G1
HWHH
Non−alert (degree)
Alert (degree)
H1
%Suppression in null direction
Non−alert (%)
Alert (%)
G2
HWHH (degree)
Alert
Non−alert
NS
H2
%Suppression in null direction
Alert
Non−alert
**

Figure 6. Population data of directional tuning properties of LGN DS cells during alert and non-alert state. **A-D,** Preferred direction responses (**A**) are significantly higher and null direction responses (**B**) are significantly lower in the alert state. **C-D,** DSIs and CVds (**D**) are higher in the alert state than in the non-alert state. **E-G,** OSIs (**E**), CVos (**F**) and HWHHs (**G**) do not change with states. **H,** Response suppression (reduction) in the null direction from the spontaneous firing rate is greater in the alert state than in the non-alert state. The cell with a negative % of suppression had an increase in the null direction response beyond spontaneous rate in the non-alert state. Population averages are shown in the bar graphs (alert in black and non-alert in white).

LGN DS simulation

The LGN DS cells code movements in the four cardinal directions with relatively broad and partially overlapped directional tuning curves (**Fig. 2H**). The main two effects of the alert state on LGN DS cells were the enhancement of visual responses in their preferred direction and the suppression of their responses in the null direction. To investigate the relative contribution of these two effects in the speed at which stimulus direction could be detected, we developed a simple model, which is illustrated in **Fig. 7A**. The firing rates of four simulated DS cells to a particular stimulus direction (Stim Direc, green arrow at left) were extracted from average tuning curves using a Poisson process. Then, the spike rates were integrated over different time windows and the integers used in a vector sum to predict the stimulus direction (PD).

Fig. 7B shows the population tuning curves in the alert (solid lines) and non-alert (dashed lines) states used to predicted three different directions 90 ˚(**Fig. 7C1**), 112.5 ˚(**Fig. 7C2**) and 135 ˚ (**Fig. 7C3**), indicated by the gray arrows above the curves. The relationships between the integration time and the mean predicted error (differences between stimulus direction and predicted direction) were obtained from the average tuning curves for the alert state (**Fig. 7C**, red), non-alert state (**Fig. 7C**, blue) and a non-alert state scaled to match the maximum response of the alert state (**Fig. 7C**, black). The contribution of response enhancement was estimated by comparing the non-alert and non-alert-scaled conditions (Gain in **Fig. 7C3**). The contribution of response suppression was estimated by comparing the alert and non-alert-scaled conditions (Suppression in **Fig. 7C3**). Interestingly, although the response enhancement seems more pronounced than the response suppression in our results (e.g. **Fig. 5C**), the contribution of both response enhancement and suppression were relatively similar. It should be noted that for all three stimulus directions tested, the integration time to get a 20 ˚mean predicted error was shorter in the alert state than in the non-alert state (mean time for Stim Direc=90 ˚in the alert vs. non-alert scaled state: 99 ± 1.7 vs. 143.5± 2.4 ms, paired t test,

p<0.001; non-alert vs. non-alert scaled state: 195.5 ± 2.7 vs. 143.5 ± 2.4 ms, paired t test, *p<0.001;* mean time for Stim Direc=112.5 ˚in the alert vs. non-alert scaled state: 123.5 ± 1.7 vs. 176.5 ± 2.2 ms, paired t test, *p<0.001*; non-alert vs. non-alert scaled state: 236.5 ± 3 vs176.5 ± 2.2 ms, paired t test, *p<0.001;* mean time for Stim Direc=135 ˚in the alert vs. non-alert scaled state: 184.5 ± 2 vs. 261.5 ± 3.4 ms, paired t test, *p<0.001*; non-alert vs. non-alert scaled state: 357.5 ± 4.6 vs. 261.5 ± 3.4 ms, paired t test, *p<0.001*). Also, the detection time was longer when the stimulus direction was least aligned with the cardinal axes for both alert and non-alert state (paired t test, *p<0.001*). Therefore, the results suggest that both the response increase in the preferred direction and response suppression in the null direction are important to enhance the signal to noise ratio and increase the speed of detection of a stimulus direction during the alert state. The simulation also predicts that stimuli moving closer to the direction of the cardinal axes will be detected faster by populations of LGN DS cells.

Figure 7

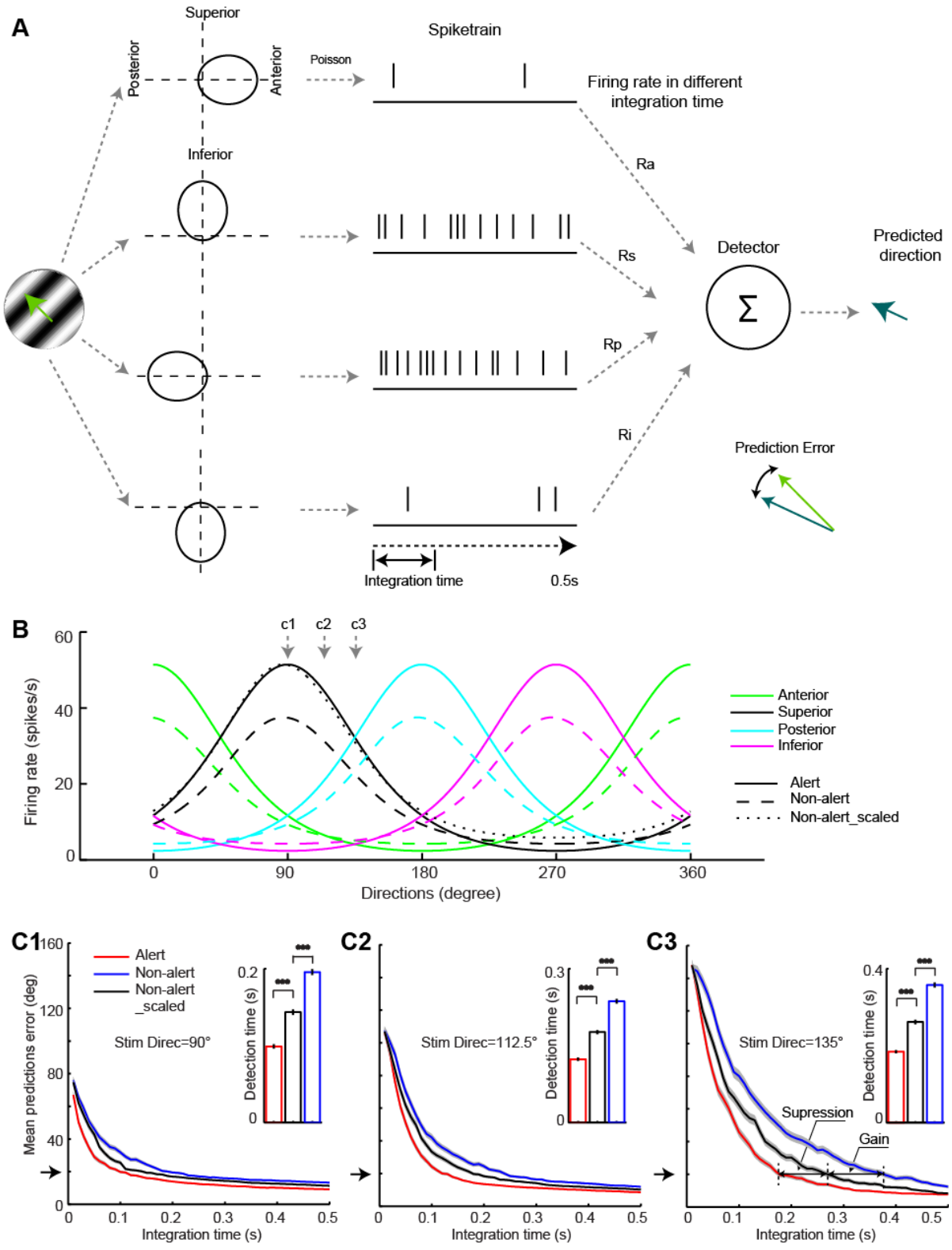
A
Superior
Posterior
Anterior
Inferior
Poisson
Spiketrain
Firing rate in different integration time
Ra
Rs
Rp
Ri
Detector
Predicted direction
Prediction Error
Integration time
0.5s
B
c1
c2
c3
Firing rate (spikes/s)
Directions (degree)
Anterior
Superior
Posterior
Inferior
Alert
Non-alert
Non-alert_scaled
C1
C2
C3
Mean predictions error (deg)
Alert
Non-alert
Non-alert _scaled
Stim Direc=90°
Stim Direc=112.5°
Stim Direc=135°
Detection time (s)
Supression
Gain
Integration time (s)

Figure 7. Simulation showing faster computation of stimulus direction in the alert state than in the non-alert state. **A,** Diagram of LGN DS model using four DS cells with preferred movements in the cardinal axes. Firing rates of the DS cells when presented with a particular stimulus direction were used to generate spike trains by Poisson process. The resulting firing rates provided inputs to a vector sum detector, using firing rates calculated in different integration times, to get the predicted direction. **B,** Population tuning curves in the alert (solid lines) and non-alert (dashed lines) state for four cells prefer movements in four cardinal directions. The tuning curve of the inferior direction (black) in the non-alert state was scaled to have the same maximum firing rate of that in the alert state, as shown in the dotted line. **C,** Relationships between integration time and mean predicted errors for three stimulus directions (Stim Direc) (90˚, 112.5˚and 135˚) in the alert (red), non-alert state (blue) and non-alert scaled state (black). Black arrows on the left show the 20˚threshold we used. Arrows in **C3** indicate the prolonged integration time due to suppression and gain, respectively. Insets: Population averages of integration time in alert, non-alert and non-alert scaled states.

Discussion

DS cells were first reported in rabbit retina > 50 years ago (Barlow and Hill, 1963) and have been also characterized in squirrels (Michael, 1966) and mice (Yoshida et al., 2001; Weng et al., 2005). Despite the relatively large proportion of retinal DS ganglion cells (18.6% -- 41% in rabbits and mice, Barlow and Hill, 1963; Barlow et al., 1964; Sun et al., 2002; Weng et al., 2005; Sun et al., 2006), LGN DS cells are more rare (Levick et al., 1969; Montero and Brugge, 1969; Swadlow and Weyand, 1985; Marshel et al., 2012; Piscopo et al., 2013), with all but one of these studies (Levick et al., 1969) reporting < 7% of LGN cells to be DS. Furthermore, DS neurons are not uniformly distributed within the LGN. Indeed, in rabbit LGN (Swadlow and Weyand, 1985; Stoelzel et al., 2008), DS neurons are much more prevalent in the representation of the upper visual field than in the representation of the visual streak (see Methods). Similarly, evidence for non-uniform distribution of DS neurons has been reported in mouse LGN (Marshel et al., 2012; Piscopo et al., 2013), which also has a visual streak-like increase in retinal ganglion cell density along the representation of the horizon (Drager and Olsen, 1981). Here, we only studied DS neurons in the LGN representation of the visual streak, in order to compare these cells with V1 simple cells studied, using the same methods, in this region of visual space (Zhuang et al., 2013; Zhuang et al., 2014).

Axonal projections of LGN DS cells

The presence of DS cells in the LGN raises questions concerning their cortical targets, and potential role in shaping the well-tuned direction/orientation selectivity seen in rabbit/rodent V1 (Piscopo et al., 2013; Scholl et al., 2013). Previous work (Swadlow and Weyand, 1985) showed that LGN DS neurons do project to V1 and that their axons have conduction velocities similar to

those of concentric LGN neurons, but the terminal layer of these axons could not determined with the antidromic methods that were employed. Preliminary studies from our lab (Hei et al., 2013) found that at least some LGN DS neurons provide a strong synaptic impact in layer 4 but, by contrast, preliminary work in mouse (Cruz-Martin et al., 2013) indicates that LGN DS neurons may selectively target superficial layers of V1. Future work will resolve this issue.

Which cells in V1 receive input from LGN DS neurons?

Orientation preference in cats and primates is columnar, and is believed to originate, in part, from selective LGN inputs with ON or OFF RF centers precisely aligned with the cortical RF subfields (Hubel and Wiesel, 1962; Tanaka, 1983; Reid and Alonso, 1995; Alonso et al., 2001; but see Mata and Ringach, 2005). By contrast, orientation selectivity in rodents and rabbits is not columnar (Drager, 1975; Bousfield, 1977; Metin et al., 1988; Girman et al., 1999; Ohki et al., 2005; Van Hooser et al., 2005; Bonin et al., 2011) and mechanism(s) generating sharp orientation/direction tuning may differ (e.g., Scholl et al., 2013). It is tempting to speculate that the DS input could contribute significantly to orientation/directional properties of simple cells. Our results, and recent findings in mouse (Piscopo et al., 2013) suggest otherwise (also see Lien and Scanziani, 2013). Thus, we found that (1) whereas LGN DS neurons have spatially overlapping ON and OFF subfields, those of simple cells are spatially segregated, (2) whereas the F1/F0 ratios of simple cells indicate a linear spatial summation, those of LGN DS cells are highly non-linear, and (3) whereas LGN DS cells have preferred directions lying on the four cardinal directions, the simple cells have more broadly distributed preferred directions. Together, these differences suggest that LGN DS neurons do not “drive” (Sherman and Guillery, 1998) V1 simple cells and convey their receptive field properties upon them.

By contrast, fast-spike inhibitory interneurons (suspected inhibitory interneurons, SINs, Swadlow and Weyand, 1987; Swadlow, 1988; Zhuang et al., 2013) are likely targets of LGN DS neurons. These cells, like the LGN DS cells, have spatial receptive fields with overlapping ON/OFF zones and very low (nonlinear) F1/F0 ratios. Notably, V1 SINs lack the directional selectivity seen in LGN DS cells. However, SINs are known to receive a convergent, promiscuous input from topographically aligned thalamic neurons that display a variety of properties. Thus, individual V1 SINs, which have overlapping ON/OFF subfields, may receive input from both ON center and OFF center LGN neurons (Zhuang et al., 2013). Moreover, SINs in layer 4 barrel cortex show little directional preference for whisker movements, but receive highly convergent input from ventrobasal thalamic neurons with a diversity of directional preferences (Swadlow and Gusev, 2002). Similar results are seen in rat barrel system (Bruno and Simons, 2002). Targeting of layer 4 SINs by LGN DS neurons would suggest a role for LGN DS neurons in driving fast and strong feed-forward inhibition that could sharpen sensory tuning of recipient simple cells, around the four cardinal directions of motion. Of course, it is also possible that LGN DS terminals in layer 4 target the descending dendrites of layer 2/3 complex cells, or ascending apical dendrites of layer 5 complex cells. Indeed, many corticotectal neurons of rabbit layer 5 have complex, directionally selective receptive fields similar to those of LGN DS neurons (Swadlow and Weyand, 1987; Swadlow, 1988). Cross-correlation studies of retinotopically aligned LGN DS neurons and cortical populations (e.g., Alonso et al., 1996, 2001; Swadlow and Gusev, 2002) would be well-suited to test these hypotheses.

Effects of Brain state on LGN DS neurons

In awake rabbits, frequent shifts between alert and non-alert brain states are associated with significant changes in spontaneous activity, burst firing (Guido and Weyand, 1995; Sherman

and Guillery, 1996; Weyand et al., 2001), and visually driven responses of LGN concentric neurons (Bezdudnaya et al., 2006; Cano et al., 2006), and some such changes are conveyed to V1 layer 4 simple cells (Bereshpolova et al., 2011; Zhuang et al., 2014). Our results in LGN DS neurons are consistent with the results for LGN concentric cells, in showing higher spontaneous firing rates, lower burst rates, and stronger responses to visual stimulation in the preferred direction when alert. Our results also show that alertness increases response suppression to stimuli moving in the null direction (Levick et al., 1969). Thus, the response enhancement in the preferred direction, and response suppression in the null direction both contribute to an increase of the signal to noise ratio when alert, even though there is no change in sharpness of tuning and direction preference (the HWHH, **Fig. 6G**). The mechanism of the enhanced null-direction suppression when alert could involve feed-forward and/or feed-back inhibition mediated by brainstem or cortical (Briggs and Usrey, 2008) inputs. However, since there is little evidence for feed-forward inhibition within rabbit LGN (Lo, 1981), the mechanism probably involves enhanced feed-back inhibition, via the thalamic reticular nucleus, and there is evidence for such arousal induced enhancement of feed-back inhibition in LGN projection cells (Swadlow and Weyand, 1985).

Functional role of LGN DS cells

Our results show that LGN DS cells provide a dedicated thalamocortical channel to transfer motion signals about the four cardinal directions to primary visual cortex. The relatively broad and overlapping directional tuning characteristics of LGN DS channels suggest that they could form the core elements of a vector-based population code for extracting directional information. We do not know the function of this thalamocortical directional information, but our simulations show how alertness could allow more rapid extraction of this information. In this regard, it is

worth noting that rabbits are frequent targets of birds of prey, that they naturally evade these predators (Pongracz and Altbacker, 1999), and that DS neurons are most prevalent in the LGN representation of the upper visual field (Swadlow and Weyand, 1985). These results and observations suggest that LGN DS cells could be useful in determining the angle of approach of areal predators, and our model and simulations indicate that alertness would hasten this computation. This would allow more rapid decisions about behavioral output (e.g., both go/no-go decisions and the direction of escape responses).

References

Alonso JM, Usrey WM, Reid RC (1996) Precisely correlated firing in cells of the lateral geniculate nucleus. Nature 383:815-819.

Alonso JM, Usrey WM, Reid RC (2001) Rules of connectivity between geniculate cells and simple cells in cat primary visual cortex. J Neurosci 21:4002-4015.

Barlow HB, Hill RM (1963) Selective sensitivity to direction of movement in ganglion cells of the rabbit retina. Science 139:412-414.

Barlow HB, Hill RM, Levick WR (1964) Retinal Ganglion Cells Responding Selectively to Direction and Speed of Image Motion in the Rabbit. J Physiol 173:377-407.

Bereshpolova Y, Stoelzel CR, Zhuang J, Amitai Y, Alonso JM, Swadlow HA (2011) Getting Drowsy? Alert/Nonalert Transitions and Visual Thalamocortical Network Dynamics. Journal of Neuroscience 31:17480-17487.

Bezdudnaya T, Cano M, Bereshpolova Y, Stoelzel CR, Alonso J-M, Swadlow HA (2006) Thalamic Burst Mode and Inattention in the Awake LGNd. Neuron 49:421-432.

Bonin V, Histed MH, Yurgenson S, Reid RC (2011) Local diversity and fine-scale organization of receptive fields in mouse visual cortex. J Neurosci 31:18506-18521.

Bousfield JD (1977) Columnar organisation and the visual cortex of the rabbit. Brain Res 136:154-158.

Briggs F, Usrey WM (2008) Emerging views of corticothalamic function. Curr Opin Neurobiol 18:403-407.

Bruno RM, Simons DJ (2002) Feedforward mechanisms of excitatory and inhibitory cortical receptive fields. J Neurosci 22:10966-10975.

Cano M, Bezdudnaya T, Swadlow HA, Alonso J-M (2006) Brain state and contrast sensitivity in the awake visual thalamus. Nature Neuroscience 9:1240-1242.

Cavanaugh J, Monosov IE, McAlonan K, Berman R, Smith MK, Cao V, Wang KH, Boyden ES, Wurtz RH (2012) Optogenetic inactivation modifies monkey visuomotor behavior. Neuron 76:901-907.

Chen Y, Anand S, Martinez-Conde S, Macknik SL, Bereshpolova Y, Swadlow HA, Alonso JM (2009) The linearity and selectivity of neuronal responses in awake visual cortex. Journal of Vision 9:12-12.

Collewijn H (1971) The optokinetic system of the rabbit. Doc Ophthalmol 30:205-226.

Cruz-Martin A, El-danaf RN, Osakada F, Nguyen PL, Callaway EM, Ghosh A, Huberman AD (2013) A 'labeled line' linking direction selective circuits in retina to superficial layers of primary visual cortex. Soc Neurosci Abst Program No. 639.07/EE6.

De Valois RL, Albrecht DG, Thorell LG (1982) Spatial frequency selectivity of cells in macaque visual cortex. Vision Res 22:545-559.

Demb JB (2007) Cellular Mechanisms for Direction Selectivity in the Retina. Neuron 55:179-186.

Drager UC (1975) Receptive fields of single cells and topography in mouse visual cortex. J Comp Neurol 160:269-290.

Drager UC, Olsen JF (1981) Ganglion cell distribution in the retina of the mouse. Invest Ophthalmol Vis Sci 20:285-293.

Elstrott J, Anishchenko A, Greschner M, Sher A, Litke AM, Chichilnisky EJ, Feller MB (2008) Direction Selectivity in the Retina Is Established Independent of Visual Experience and Cholinergic Retinal Waves. Neuron 58:499-506.

Fried SI, Munch TA, Werblin FS (2002) Mechanisms and circuitry underlying directional selectivity in the retina. Nature 420:411-414.

Fried SI, Munch TA, Werblin FS (2005) Directional selectivity is formed at multiple levels by laterally offset inhibition in the rabbit retina. Neuron 46:117-127.

Girman SV, Sauve Y, Lund RD (1999) Receptive field properties of single neurons in rat primary visual cortex. J Neurophysiol 82:301-311.
Grabska-Barwinska A, Ng BS, Jancke D (2012) Orientation selective or not? - Measuring significance of tuning to a circular parameter. J Neurosci Methods 203:1-9.
Guido W, Weyand T (1995) Burst responses in thalamic relay cells of the awake behaving cat. J Neurophysiol 74:1782-1786.
Hei X, Stoelzel CR, Zhuang J, Bereshpolova Y, Huff JM, Alonso JM, Swadlow HA (2013) Directional selective neurons in rabbit LGNd project to layer 4 of V1 and are modulated by brain state. Soc Neurosci Abst Program No. 737.13/JJ5.
Hubel DH, Wiesel TN (1962) Receptive fields, binocular interaction and functional architecture in the cat's visual cortex. J Physiol 160:106-154.
Huberman AD, Wei W, Elstrott J, Stafford BK, Feller MB, Barres BA (2009) Genetic Identification of an On-Off Direction- Selective Retinal Ganglion Cell Subtype Reveals a Layer-Specific Subcortical Map of Posterior Motion. Neuron 62:327-334.
Hughes A (1971) Topographical relationships between the anatomy and physiology of the rabbit visual system. Doc Ophthalmol 30:33-159.
Jones JP, Palmer LA (1987) The two-dimensional spatial structure of simple receptive fields in cat striate cortex. J Neurophysiol 58:1187-1211.
Levick WR, Oyster CW, Takahashi E (1969) Rabbit lateral geniculate nucleus: sharpener of directional information. Science 165:712-714.
Lien AD, Scanziani M (2013) Tuned thalamic excitation is amplified by visual cortical circuits. Nat Neurosci 16:1315-1323.
Lo FS (1981) Synaptic organization of the lateral geniculate nucleus of the rabbit: lack of feed-forward inhibition. Brain Res 221:387-392.
Marshel James H, Kaye Alfred P, Nauhaus I, Callaway Edward M (2012) Anterior-Posterior Direction Opponency in the Superficial Mouse Lateral Geniculate Nucleus. Neuron 76:713-720.
Mata ML, Ringach DL (2005) Spatial overlap of ON and OFF subregions and its relation to response modulation ratio in macaque primary visual cortex. J Neurophysiol 93:919-928.
Metin C, Godement P, Imbert M (1988) The primary visual cortex in the mouse: receptive field properties and functional organization. Exp Brain Res 69:594-612.
Michael CR (1966) Receptive fields of directionally selective units in the optic nerve of the ground squirrel. Science 152:1092-1095.
Montero VM, Brugge JF (1969) Direction of movement as the significant stimulus parameter for some lateral geniculate cells in the rat. Vision Res 9:71-88.
Movshon JA, Thompson ID, Tolhurst DJ (1978) Spatial summation in the receptive fields of simple cells in the cat's striate cortex. J Physiol 283:53-77.
Oesch N, Euler T, Taylor WR (2005) Direction-Selective Dendritic Action Potentials in Rabbit Retina. Neuron 47:739-750.
Ohki K, Chung S, Ch'ng YH, Kara P, Reid RC (2005) Functional imaging with cellular resolution reveals precise micro-architecture in visual cortex. Nature 433:597-603.
Oyster CW, Barlow HB (1967) Direction-selective units in rabbit retina: distribution of preferred directions. Science 155:841-842.
Piscopo DM, El-Danaf RN, Huberman AD, Niell CM (2013) Diverse Visual Features Encoded in Mouse Lateral Geniculate Nucleus. Journal of Neuroscience 33:4642-4656.
Pongracz P, Altbacker V (1999) The effect of early handling is dependent upon the state of the rabbit (Oryctolagus cuniculus) pups around nursing. Dev Psychobiol 35:241-251.
Reid RC, Alonso JM (1995) Specificity of monosynaptic connections from thalamus to visual cortex. Nature 378:281-284.
Ringach DL, Shapley RM, Hawken MJ (2002) Orientation selectivity in macaque V1: diversity and laminar dependence. J Neurosci 22:5639-5651.

Scholl B, Tan AY, Corey J, Priebe NJ (2013) Emergence of orientation selectivity in the Mammalian visual pathway. J Neurosci 33:10616-10624.
Sherman SM, Guillery RW (1996) Functional organization of thalamocortical relays. J Neurophysiol 76:1367-1395.
Sherman SM, Guillery RW (1998) On the actions that one nerve cell can have on another: distinguishing "drivers" from "modulators". Proc Natl Acad Sci U S A 95:7121-7126.
Simpson JI (1984) The accessory optic system. Annu Rev Neurosci 7:13-41.
Stewart DL, Chow KL, Masland RH (1971) Receptive-field characteristics of lateral geniculate neurons in the rabbit. J Neurophysiol 34:139-147.
Stoelzel CR, Bereshpolova Y, Gusev AG, Swadlow HA (2008) The Impact of an LGNd Impulse on the Awake Visual Cortex: Synaptic Dynamics and the Sustained/Transient Distinction. Journal of Neuroscience 28:5018-5028.
Sun W, Li N, He S (2002) Large-scale morphological survey of mouse retinal ganglion cells. J Comp Neurol 451:115-126.
Sun W, Deng Q, Levick WR, He S (2006) ON direction-selective ganglion cells in the mouse retina. The Journal of Physiology 576:197-202.
Swadlow HA (1988) Efferent neurons and suspected interneurons in binocular visual cortex of the awake rabbit: receptive fields and binocular properties. J Neurophysiol 59:1162-1187.
Swadlow HA (1991) Efferent neurons and suspected interneurons in second somatosensory cortex of the awake rabbit: receptive fields and axonal properties. J Neurophysiol 66:1392-1409.
Swadlow HA (2005) A Multi-Channel, Implantable Microdrive System for Use With Sharp, Ultra-Fine "Reitboeck" Microelectrodes. Journal of Neurophysiology 93:2959-2965.
Swadlow HA, Weyand TG (1985) Receptive-field and axonal properties of neurons in the dorsal lateral geniculate nucleus of awake unparalyzed rabbits. J Neurophysiol 54:168-183.
Swadlow HA, Weyand TG (1987) Corticogeniculate neurons, corticotectal neurons, and suspected interneurons in visual cortex of awake rabbits: receptive-field properties, axonal properties, and effects of EEG arousal. J Neurophysiol 57:977-1001.
Swadlow HA, Gusev AG (2002) Receptive-field construction in cortical inhibitory interneurons. Nat Neurosci 5:403-404.
Swadlow HA, Beloozerova IN, Sirota MG (1998) Sharp, local synchrony among putative feed-forward inhibitory interneurons of rabbit somatosensory cortex. J Neurophysiol 79:567-582.
Tanaka K (1983) Cross-correlation analysis of geniculostriate neuronal relationships in cats. J Neurophysiol 49:1303-1318.
Van Hooser SD, Heimel JA, Chung S, Nelson SB, Toth LJ (2005) Orientation selectivity without orientation maps in visual cortex of a highly visual mammal. J Neurosci 25:19-28.
Weng S, Sun W, He S (2005) Identification of ON-OFF direction-selective ganglion cells in the mouse retina. J Physiol 562:915-923.
Weyand TG, Boudreaux M, Guido W (2001) Burst and tonic response modes in thalamic neurons during sleep and wakefulness. J Neurophysiol 85:1107-1118.
Yoshida K, Watanabe D, Ishikane H, Tachibana M, Pastan I, Nakanishi S (2001) A key role of starburst amacrine cells in originating retinal directional selectivity and optokinetic eye movement. Neuron 30:771-780.
Zhuang J, Stoelzel CR, Bereshpolova Y, Huff JM, Hei X, Alonso JM, Swadlow HA (2013) Layer 4 in primary visual cortex of the awake rabbit: contrasting properties of simple cells and putative feedforward inhibitory interneurons. J Neurosci 33:11372-11389.
Zhuang J, Bereshpolova Y, Stoelzel CR, Huff JM, Hei X, Alonso JM, Swadlow HA (2014) Brain state effects on layer 4 of the awake visual cortex. J Neurosci 34:3888-3900.